PHYSICS

Iran J Radiol. 2016 January; 13(1): e18217. doi: 10.5812/iranjradiol.18217

Published online 2016 January 2. **Research Article**

Effects of Variations of Flow and Heart Rate on Intra-Aneurysmal Hemodynamics in a Ruptured Internal Carotid Artery Aneurysm During Exercise

Ali Sarrami-Foroushani,[1] Mohsen Nasr Esfahany,[1,*] Hamidreza Saligheh Rad,[2] Kavous Firouznia,[3] Madjid Shakiba,[3] and Hossein Ghanaati[3]

[1]Department of Chemical Engineering, Isfahan University of Technology, Isfahan, Iran
[2]Medical Physics and Biomedical Engineering, Tehran University of Medical Sciences, Tehran, Iran
[3]Advanced Diagnostic and Interventional Radiology Research Center (ADIR), Tehran University of Medical Sciences, Tehran, Iran

*Corresponding author: Mohsen Nasr Esfahany, Department of Chemical Engineering, Isfahan University of Technology, Isfahan, Iran. Tel: +98-3133915631, Fax: +98-3113912677, E-mail: mnasr@cc.iut.ac.ir

Received 2014 February 13; **Revised** 2014 June 18; **Accepted** 2014 July 20.

Abstract

Background: Hemodynamics is thought to play an important role in the mechanisms responsible for initiation, growth, and rupture of intracranial aneurysms. Computational fluid dynamic (CFD) analysis is used to assess intra-aneurysmal hemodynamics.

Objectives: This study aimed to investigate the effects of variations in heart rate and internal carotid artery (ICA) flow rate on intra-aneurysmal hemodynamics, in an ICA aneurysm, by using computational fluid dynamics.

Patients and Methods: Computed tomography angiography (CTA) was performed in a 55 years old female case, with a saccular ICA aneurysm, to create a patient-specific geometrical anatomic model of the aneurysm. The intra-aneurysmal hemodynamic environments for three states with different flow and heart rates were analyzed using patient-specific image-based CFD modeling.

Results: Results showed significant changes for the three simulated states. For a proportion of the states examined, results were counterintuitive. Systolic and time-averaged wall shear stress and pressure on the aneurysm wall showed a proportional evolution with the mainstream flow rate.

Conclusion: Results reinforced the pivotal role of vascular geometry, with respect to hemodynamics, together with the importance of performing patient-specific CFD analyses, through which the effect of different blood flow conditions on the aneurysm hemodynamics could be evaluated.

Keywords: Fluid Dynamics, Internal Carotid Artery, Aneurysm, Heart Rate

1. Background

An aneurysm is a vascular condition characterized by localized dilatation of arterial walls, which is inherently carrying a risk of rupture and hemorrhage. Intracranial aneurysms tend to occur near arterial bifurcations, around the Circle of Willis, and their rupture leads to subarachnoid hemorrhage (SAH), which is associated with high rates of mortality and morbidity. Adverse hemodynamics is thought to play a vital role in the mechanisms responsible for initiation, growth, and rupture of aneurysms. Therefore, a hemodynamics assessment, before planning possible therapies, is very important for clinicians in order to reduce intervention risks in favor of benefits. In the past few years, patient-specific image-based computational fluid dynamics (CFD) has been used as a powerful technique to study blood flow behavior in vessels, in order to understand mechanisms of cardiovascular and cerebrovascular diseases. The CFD has been employed to evaluate several hemodynamic parameters, such as blood velocity, blood pressure, wall shear stress (WSS), and turbulence intensity, which are accepted to play role in development, diagnosis, and treatment of vascular diseases (1-7). As a simulation technique, CFD needs: 1) three-dimensional (3D) vessel anatomical model (geometry), which is commonly reconstructed from computed tomography angiography (CTA), magnetic resonance angiography (MRA), or 3D rotational angiography (3DRA); 2) models to predict blood transport properties, 3) blood flow or pressure waveforms at inlets and outlets of the vascular bed to be simulated, which are assigned as inlet and outlet boundary conditions and are commonly assumed or occasionally obtained from patient-specific measurements. Among the studies in this field, a number of researchers have investigated the role of hemodynamics in initiation (8-10), growth (11, 12), and rupture (6, 13, 14) of aneurysms. Hemodynamic stresses are accepted to play an important role in aneurysm initiation, growth, and rupture. The WSS and tensile stress is two of these

stresses. The former, which is associated with viscous fluid flow induced frictional force on the wall, acts as a mechanical signal to the endothelial cells responsible for vascular remodeling and modulates their function, while the latter is associated with blood pressure and stimulates collagen synthesis and degradation. Although intra-aneurysmal hemodynamic environment interacts with aneurysm wall through both WSS and pressure, WSS are thought to play a more important role in aneurysm growth and rupture (3). Therefore, assessment of WSS and other hemodynamic parameters related to it have been suggested to evaluate risk of rupture in aneurysms (6). Bowker et al. (15), Les et al. (16), and Suh et al. (17) studied the effects of exercise on intra-aneurysmal hemodynamics and observed that WSS on the aneurysm increased during exercise. However, Bowker et al. (15) studied only middle cerebral artery aneurysms, while the other two focused on abdominal aortic aneurysms.

2. Objectives

This paper will use patient-specific CFD technique to simulate intra-aneurysmal hemodynamics in an aneurysm located on terminal internal carotid artery (ICA) and perform both qualitative and quantitative studies on the effects of blood flow and heart rate alterations during exercise on the hemodynamic behavior of this aneurysm.

3. Patients and Methods

CTA was performed on a 55 years old female with a saccular aneurysm in the ICA, on GE Lightspeed VCT 64-slice scanner (General Electric Healthcare, Milwaukee, WI, USA) in Imam Khomeini Hospital, Tehran, Iran. A 3D patient-specific geometric model of the aneurysm was constructed after segmentation of 3D CTA images in Materialise MIMICS (Materialise NV, Leuven, Belgium) (Figure 1). The geometric model is then used to generate a volumetric computational unstructured mesh of 2795046 elements in ANSYS ICEM CFD (Ansys Inc., Canonsburg, PA, USA). Blood flow was modeled by unsteady 3D Navier-Stokes equations for incompressible Newtonian fluid. Blood is assumed to be a homogeneous Newtonian fluid of density 1066 kg/m^3 and viscosity 0.0035 Pa·s. The assumption of blood, as a Newtonian fluid, is demonstrated to be reasonable in large vessels with high shear rate (18). Despite compliance of the vessel walls, due to the lack of elastin in cerebral arteries (19), vessels were assumed to be rigid, with a no slip boundary condition at walls. Pressure waveforms, obtained from one-dimensional global analysis of systemic arterial tree (20), were prescribed as the outlet boundary conditions at the outlets, i.e. anterior communicating artery (ACA) and middle cerebral artery (MCA).

Sato and Sadamoto (21) measured the variations of blood flow and heart rate in ICA, during dynamic exercise. To study the effect of entering flow on intra-aneurysmal hemodynamics, three different states, with different inlet flow and heart rates, were simulated (Table 1). A flow waveform, obtained from 1D model of systemic

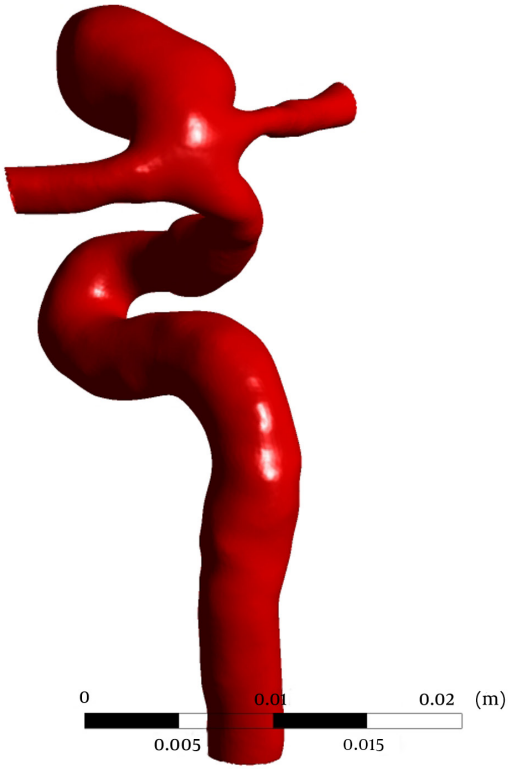

Figure 1. Reconstructed 3D model used for CFD Simulations

Table 1. Heart Rate and Changes in Internal Carotid Artery Flow Rate in Each of the Three States[a]

	State 1, Rest	State 2	State 3
Heart rate, beats/min	60	93	127
Change in ICA flow rate, %	-	11.6	18.4

[a]Abbreviation: ICA, internal carotid artery

arterial tree (20), was used as the inlet boundary condition at state 1 (at rest) and modulated according to Sato and Sadamoto measurements, to generate inlet boundary conditions for the other two states and mimic the effects of exercise on intra-aneurysmal hemodynamics. Mean arterial-level WSS needed to maintain the structure of the arterial vessels is 1.5 Pa (22). Inlet flow waveform is scaled with the inlet area, to maintain a mean WSS of 1.5 Pa at the inlet (23). The CFD simulations were run using ANSYS-CFX® (Ansys Inc. Canonsburg, PA, USA) for three cardiac cycles, with a time step of 0.005 seconds and the results obtained at the third cardiac cycle were reported. A straight tube extension, proximal to the real inlet, was used to ensure that the blood flow entering the main computational domain has a fully-developed velocity profile.

4. Results

Blood flow in the aneurysm was simulated at three states (Table 1). Effects of variations in blood flow and heart rate on intra-aneurysmal hemodynamics were compared qualitatively and quantitatively, for different states.

4.1. Qualitative Comparison

Distributions of WSS, time-averaged over a cardiac cycle on the aneurysmal wall, are shown in Figure 2 for the three states (first row). For all states, areas of elevated WSS were observed around the aneurysm neck and the remainder of the aneurysm wall was exposed to low WSS. Visual comparison of the states showed an increase in WSS in state 2, compared to state 1, whereas time-averaged WSS decreased in state 3, although blood flow and heart rate were increased in this state. Figure 2 also shows the distribution of WSS on the aneurysm region at peak systole, for each state. Systolic WSS, however, increased, as flow and heart rate increased in all states.

Figure 3 depicts the distribution of aneurysmal wall pressure at peak systole. An impingement region, concentrated at the aneurysm neck, was observed for all states (marked by a small ball on Figure 3). The location of impingement region slightly changed in state 3 and interestingly, in state 2, the maximum pressure at the aneurysm neck and also the pressure on the aneurysm apex were higher than the two other states. There is an area of elevated pressure on the aneurysm apex in states 1 and 2, which has disappeared in state 3.

Figure 4 shows the isovelocity surfaces corresponding to 22 cm/second, at peak systole. One can see a stronger impinging jet into the aneurysm in state 1. This stronger impinging jet explains the higher aneurysm wall systolic pressure in this state of flow and heart rate.

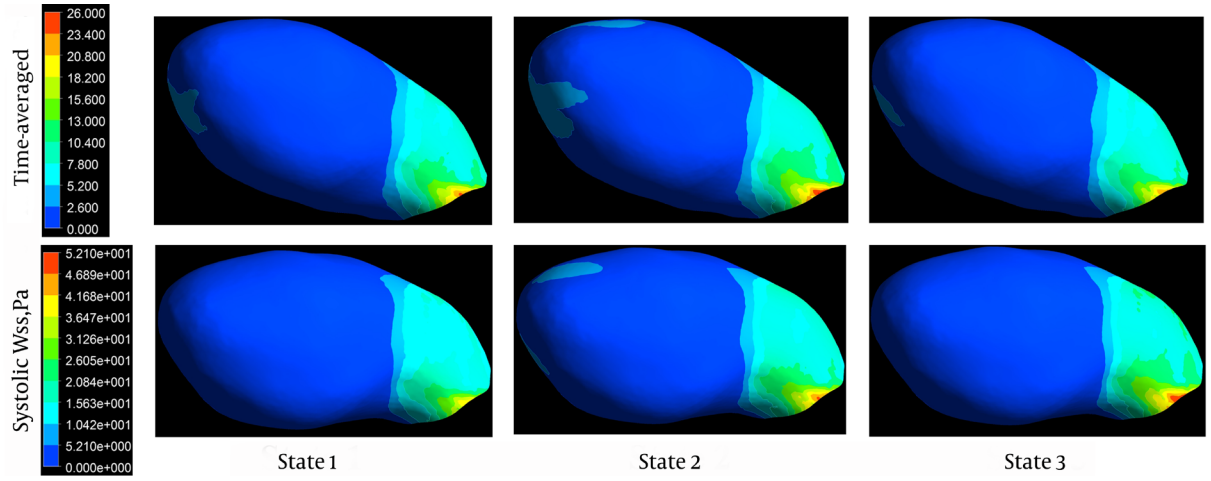

Figure 2. Wall shear stress distributions for three states time-averaged over a cardiac cycle (first row) and at peak systole (second row).

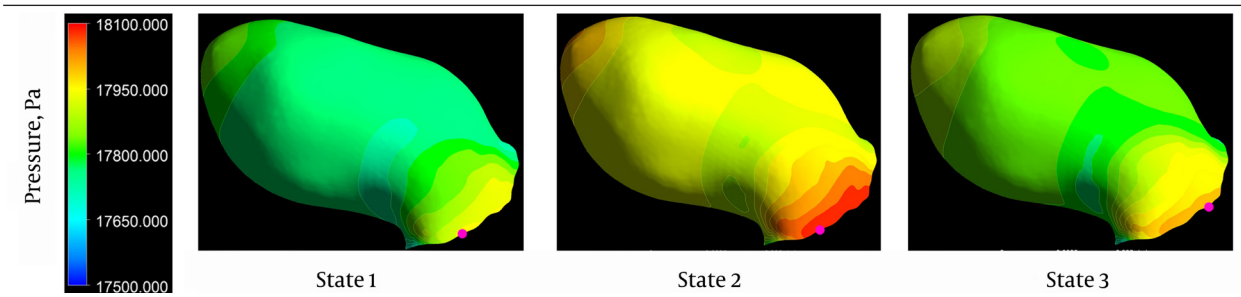

Figure 3. Pressure distributions for three states at peak systole. The impingement point is shown by a small violet ball on each contour.

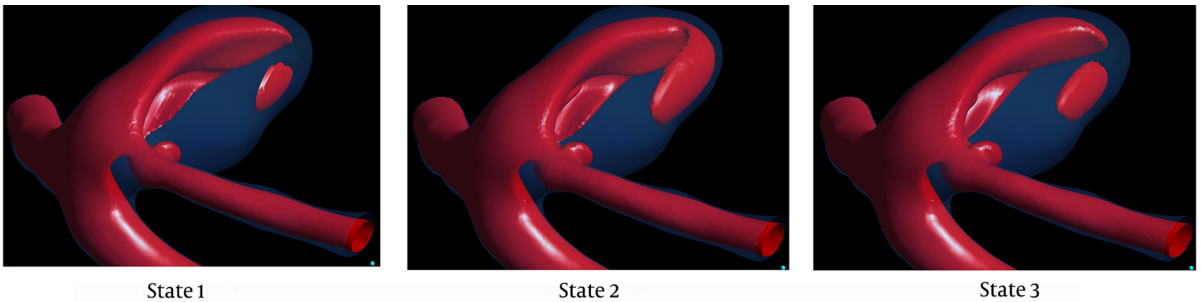

Figure 4. Isovelocity surfaces corresponding to 22 cm/secend for three states at peak systole

The oscillatory shear index (OSI) is a biomechanical parameter that shows the flow oscillations along a cardiac cycle. It is related to the ratio of magnitude of time-averaged WSS vector to the time-averaged WSS magnitude. By monitoring the differences between magnitude of the time-averaged WSS and time-averaged magnitude of WSS, OSI indicates the WSS vector deflection from blood flow predominant direction. The OSI values can vary between 0 for no variations in WSS vector to 0.5 for 180° deflection of WSS direction. The OSI is calculated based on equation 1.

$$\text{OSI} = \frac{1}{2} \times \left(1.0 - \frac{\int_0^T \vec{\text{WSS}}}{\int_0^T \vec{\text{WSS}}} \right) \quad (1)$$

Distributions of OSI on the aneurysm wall are shown in Figure 5. Visual comparison of the contour maps reveals that states with higher flow rates are associated with smaller areas of elevated WSS. Nevertheless, OSI contours are of approximately the same pattern in all states and, as expected, the areas of elevated OSI are concentrated at the regions where the WSS is low.

4.2. Quantitative Comparison

The WSS and pressure, averaged temporally, over a cardiac cycle, and spatially, over the aneurysm wall, as well as maximum WSS and pressure on the aneurysm wall, averaged over a cardiac cycle, are presented in Table 2 for all three states. One can see that in states 2 and 3, when the flow and heart rate are greater than in state 1, the vessel lumen is exposed to greater averaged values of WSS and pressure, on a cardiac cycle. However, as previously observed qualitatively, maximum pressure on the aneurysm region at peak systole in state 2 is, counter-intuitively, 0.5% (100 Pa) greater than state 3, where the flow and heart rates are greater than state 2. Nevertheless, this difference is really negligible and one can say that there is almost no change on aneurysm wall pressure moving from state 1 to states 2 and 3. On the other hand, relatively high-pressure impingement region area in state 1 is 4% of the whole aneurysm, while this value slightly increased to 4.3% in state 2, and decreased to 3.1% in state 3, with greater flow rates than state 1. Area of elevated WSS in state 1 is 1%, which, in states 2 and 3, grew to be 1.2% of the whole aneurysmal wall area.

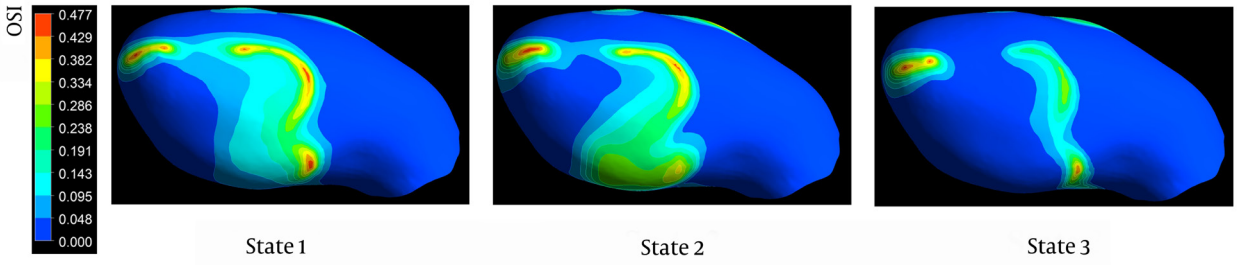

Figure 5. Distributions of oscillatory stress index for three states

Table 2. Changes in Space and Time Averaged, and Time-Averaged Maximum Wall Shear Stress and Pressure on the Aneurysmal Wall for Three Analyzed States[a]

	State 1	State 2	State 3
Space and Time Averaged WSS on the Aneurysm Wall, Pa	2.33	2.65	2.23
Change from State 1, %		13.7	-4.4
Time Averaged Maximum WSS on the Aneurysm Wall, Pa	25.05	29.24	31.67
Change from State 1, %		16.7	26.4
Space and Time Averaged Pressure on the Aneurysm Wall, Pa	12961.21	12998.54	12999.31
Change from State 1, %		0.3	0.3
Time Averaged Maximum Pressure on the Aneurysm Wall, Pa	13032.97	13087.36	13098.94
Change from State 1, %		0.4	0.5

[a]Abbreviation: WSS, wall shear stress.

Both high and low WSS have been found to be correlated with aneurysm growth and rupture (3). To follow the implications of this finding, areas of aneurysm wall regions exposed to time-averaged WSS greater than 1.5 Pa and lower than 0.4 Pa are studied. The simulations showed that 13.4% and 42.6% of the whole aneurysm wall are exposed to time-averaged WSS below 0.4 Pa and above 1.5 Pa, respectively. As expected, in state 2, an increase in blood flow rate compared to state 1 caused areas with time-averaged WSS below 0.4 Pa to decrease to 8.3% and areas with time-averaged WSS greater than 1.5 Pa to increase to 49.6% of the whole aneurysm wall area. In contrast, while flow rate is increased in state 3, areas with time-averaged WSS below 0.4 Pa increased to 17.3% and areas with time-averaged WSS above 1.5 Pa decreased to 42.8% of the whole aneurysm wall area. These counter-intuitive results indicate the role of complex intra-aneurysmal hemodynamics on parameters thought to be important in aneurysm rupture.

5. Discussion

Results of patient-specific image-based CFD analysis of the intra-aneurysmal hemodynamics performed on a ruptured ICA aneurysm showed significant changes for the three simulated states. However, for several of the parameters examined, results were counter-intuitive.

Velocity vector field, as the most important hemodynamic variable, which is used to establish WSS and pressure on the aneurysmal wall, could be alternatively obtained from CFD or imaging techniques, such as Phase-Contrast Magnetic Resonance Imaging (PC MRI); however, PC MRI is only applicable on vessels with simple structures and large diameter, and fails to map rotational and secondary slow flows with acceptable resolution. The CFD analysis, instead, was demonstrated to be able to visualize and quantify hemodynamic parameters, with high resolution.

In this work, effects of variations of ICA flow rates on intra-aneurysmal hemodynamics were studied, using hemodynamic parameters, such as WSS, pressure, and areas of elevated and low WSS. Blood pressure, which is translated to a tensile stress in the wall, affects the vessel lumen via stimulation of cell-mediated collagen synthesis and cross-linking and collagen degradation. On the other hand, WSS, as a mechanical signal, is sensed and transduced to biologic signals by endothelial cells, which activate the biomechanical pathways that maintain vascular homeostasis and regulate remodeling (6). Blood pressure and WSS are both thought to play an important role in aneurysm pathobiology; however, collagen turnover, as a biological response to imbalanced wall tensile stresses, reduces the imbalance itself and mitigate the effect of blood pressure. Hence, WSS-mediated effects received more clinical attention. It is showed that a WSS of around 2.0 Pa is suitable for maintaining the vessel structure while low WSS may lead to endothelial cell degeneration, via apoptotic cell cycle (20). Current study examined the effects of variations in ICA flow rate on areas of elevated and low WSS and revealed intuitive results of increasing WSS on aneurysm wall with increasing blood flow and heart rate. However, several counter-intuitive trends were observed in areas of excessively low WSS and elevated WSS in state 3, which accentuates the pivotal role of CFD in reporting and predicting aneurysms development. Still, the present study outlines the importance of performing patient-specific CFD analyses for blood flow in aneurysms, which may assist the clinical decision making in selecting an efficient treatment plan for each individual case. Rigid walls assumption and treating blood as a Newtonian fluid are the limitations of this study, which are common in most CFD simulations in the field. As previously mentioned these assumptions were investigated in (18, 19) and have been shown to have negligible effects while CFD analysis is employed to quantify flow patterns and main hemodynamic measures in intracranial aneurysms.

To conclude, the results of this study reinforced the pivotal role of vascular geometry with respect to hemodynamics, together with the importance of performing patient-specific CFD analyses, through which the effect of different blood flow conditions on the aneurysm hemodynamics could be evaluated.

Acknowledgments

There are no additional contributions outside the ones of the article authors.

Footnotes

Authors' Contributions: Study concept and design: Ali Sarrami-Foroushani, Mohsen Nasr Esfahany, Hamidreza Saligheh Rad, Madjid Shakiba, Kavous Firouznia and Hossein Ghanaati. Acquisition of data: Madjid Shakiba, and Kavous Firouznia. Analysis and Interpretation of data: Ali Sarrami-Foroushani, and Mohsen Nasr Esfahany. Drafting the manuscript: Ali Sarrami-Foroushani. Critical revision of the manuscript for important intellectual content: Mohsen Nasr-Esfahany, Hamidreza Saligheh Rad, Kavous Firouznia, and Madjid Shakiba. Administrative, technical and material support: Mohsen Nasr-Esfahany, Hamidreza Saligheh Rad, Kavous Firouznia, and Hossein Ghanaati. Study supervision: Mohsen Nasr Esfahany, Hamidreza Saligheh Rad, and Kavous Firooznia.

Financial Disclosure: The authors declare that there is no competing financial interests and grant support.

Funding/Support: This study was not supported research funding.

References

1. Meng H, Tutino VM, Xiang J, Siddiqui A. High WSS or low WSS? Complex interactions of hemodynamics with intracranial aneurysm initiation, growth, and rupture: toward a unifying hypothesis. *AJNR Am J Neuroradiol.* 2014;**35**(7):1254–62. doi: 10.3174/ajnr.A3558. [PubMed: 23598838]

2. Meng H, Mocco J, Siddiqui A, Mandelbaum M, Kolega J, Xiang J, et al. High Wall Shear Stress and Positive Wall Shear Stress Gradient Trigger the Initiation of Intracranial Aneurysms. *Am Soc Mech Eng.* 2009:523–4. doi: 10.1115/sbc2009-206395.
3. Xiang J, Tutino VM, Snyder KV, Meng H. CFD: Computational fluid dynamics or confounding factor dissemination? The role of hemodynamics in intracranial aneurysm rupture risk assessment. *Am J Neuroradiology.* 2014;**35**(10):1849–57. doi: 10.3174/ajnr.A3710.
4. Arzani A, Dyverfeldt P, Ebbers T, Shadden SC. In vivo validation of numerical prediction for turbulence intensity in an aortic coarctation. *Ann Biomed Eng.* 2012;**40**(4):860–70. doi: 10.1007/s10439-011-0447-6. [PubMed: 22016327]
5. Nixon AM, Gunel M, Sumpio BE. The critical role of hemodynamics in the development of cerebral vascular disease. *J Neurosurg.* 2010;**112**(6):1240–53. doi: 10.3171/2009.10.JNS09759. [PubMed: 19943737]
6. Shojima M, Oshima M, Takagi K, Torii R, Hayakawa M, Katada K, et al. Magnitude and role of wall shear stress on cerebral aneurysm: computational fluid dynamic study of 20 middle cerebral artery aneurysms. *Stroke.* 2004;**35**(11):2500–5. doi: 10.1161/01.STR.0000144648.89172.0f. [PubMed: 15514200]
7. Sforza DM, Putman CM, Cebral JR. Hemodynamics of Cerebral Aneurysms. *Annu Rev Fluid Mech.* 2009;**41**:91–107. doi: 10.1146/annurev.fluid.40.111406.102126. [PubMed: 19784385]
8. Baek H, Jayaraman MV, Karniadakis GE. Wall shear stress and pressure distribution on aneurysms and infundibulae in the posterior communicating artery bifurcation. *Ann Biomed Eng.* 2009;**37**(12):2469–87. doi: 10.1007/s10439-009-9794-y. [PubMed: 19757058]
9. Mantha A, Karmonik C, Benndorf G, Strother C, Metcalfe R. Hemodynamics in a cerebral artery before and after the formation of an aneurysm. *AJNR Am J Neuroradiol.* 2006;**27**(5):1113–8. [PubMed: 16687554]
10. Kulcsar Z, Ugron A, Marosfoi M, Berentei Z, Paal G, Szikora I. Hemodynamics of cerebral aneurysm initiation: the role of wall shear stress and spatial wall shear stress gradient. *AJNR Am J Neuroradiol.* 2011;**32**(3):587–94. doi: 10.3174/ajnr.A2339. [PubMed: 21310860]
11. Kroon M, Holzapfel GA. Modeling of saccular aneurysm growth in a human middle cerebral artery. *J Biomech Eng.* 2008;**130**(5):051012. doi: 10.1115/1.2965597. [PubMed: 19045519]
12. Boussel L, Rayz V, McCulloch C, Martin A, Acevedo-Bolton G, Lawton M, et al. Aneurysm growth occurs at region of low wall shear stress: patient-specific correlation of hemodynamics and growth in a longitudinal study. *Stroke.* 2008;**39**(11):2997–3002. doi: 10.1161/STROKEAHA.108.521617. [PubMed: 18688012]
13. Jou LD, Lee DH, Morsi H, Mawad ME. Wall shear stress on ruptured and unruptured intracranial aneurysms at the internal carotid artery. *AJNR Am J Neuroradiol.* 2008;**29**(9):1761–7. doi: 10.3174/ajnr.A1180. [PubMed: 18599576]
14. Cebral JR, Mut F, Weir J, Putman C. Quantitative characterization of the hemodynamic environment in ruptured and unruptured brain aneurysms. *AJNR Am J Neuroradiol.* 2011;**32**(1):145–51. doi: 10.3174/ajnr.A2419. [PubMed: 21127144]
15. Bowker TJ, Watton PN, Summers PE, Byrne JV, Ventikos Y. Rest versus exercise hemodynamics for middle cerebral artery aneurysms: a computational study. *AJNR Am J Neuroradiol.* 2010;**31**(2):317–23. doi: 10.3174/ajnr.A1797. [PubMed: 19959776]
16. Les AS, Shadden SC, Figueroa CA, Park JM, Tedesco MM, Herfkens RJ, et al. Quantification of hemodynamics in abdominal aortic aneurysms during rest and exercise using magnetic resonance imaging and computational fluid dynamics. *Ann Biomed Eng.* 2010;**38**(4):1288–313. doi: 10.1007/s10439-010-9949-x. [PubMed: 20143263]
17. Suh GY, Les AS, Tenforde AS, Shadden SC, Spilker RL, Yeung JJ, et al. Hemodynamic changes quantified in abdominal aortic aneurysms with increasing exercise intensity using mr exercise imaging and image-based computational fluid dynamics. *Ann Biomed Eng.* 2011;**39**(8):2186–202. doi: 10.1007/s10439-011-0313-6. [PubMed: 21509633]
18. Nichols WW, O'Rourke MF. McDonald's blood flow in arteries: theoretical, experimental, and clinical principles:. CRC Press; 2011.
19. Humphrey JD, Na S. Elastodynamics and arterial wall stress. *Ann Biomed Eng.* 2002;**30**(4):509–23. [PubMed: 12086002]
20. Reymond P, Merenda F, Perren F, Rufenacht D, Stergiopulos N. Validation of a one-dimensional model of the systemic arterial tree. *Am J Physiol Heart Circ Physiol.* 2009;**297**(1):H208–22. doi: 10.1152/ajpheart.00037.2009. [PubMed: 19429832]
21. Sato K, Sadamoto T. Different blood flow responses to dynamic exercise between internal carotid and vertebral arteries in women. *J Appl Physiol (1985).* 2010;**109**(3):864–9. doi:10.1152/japplphysiol.01359.2009. [PubMed: 20595539]
22. Malek AM, Alper SL, Izumo S. Hemodynamic shear stress and its role in atherosclerosis. *JAMA.* 1999;**282**(21):2035–42. [PubMed: 10591386]
23. Cebral JR, Castro MA, Putman CM, Alperin N. Flow-area relationship in internal carotid and vertebral arteries. *Physiol Meas.* 2008;**29**(5):585–94. doi: 10.1088/0967-3334/29/5/005. [PubMed: 18460763]